Ponderomotive generation of density cavities from kinetic Alfvén wave–slow-mode coupling in Earth's high-β plasma sheet

Mani K Chettri[1] Hemam D. Singh[2] Rupak Mukherjee[1]

[1]Sikkim University, Gangtok, India [2]Netaji Subhas University of Technology, New Delhi, India

KAW–slow-mode ponderomotive coupling ⇒ long-lived, ion-scale density holes.

1. Motivation

- Kinetic Alfvén waves (KAWs) carry electromagnetic energy in the collisionless, **high-β magnetotail plasma sheet**, where compressive responses are strong.
- **Question:** can the *nonlinear ponderomotive* coupling of a dispersive KAW to a slow-mode density perturbation generate the **localized density cavities** / **magnetic-hole-like structures** seen in the plasma sheet and its boundary layer (PSBL)?
- We model this with a reduced two-fluid **Zakharov-type** system and compare with MMS data and with published Cluster, Polar and Freja results.

2. Reduced two-fluid model (Zakharov-type)

Dispersive KAW field $b = \delta B_y/B_0$ refractively coupled to the slow density $\eta = n/n_0$, the ion-acoustic response, "slow" relative to the KAW oscillation (ion-sound gyroradius dispersion $\alpha = (\rho_s/L_\perp)^2$, $\mu = (c_s/v_A)^2 = \beta/2$, aspect ratio $\lambda = L_\parallel/L_\perp$):

$$\partial_{tt} b - \partial_{zz}\big(1 - \alpha\,\partial_{xx}\big) b + \partial_z(\eta\,\partial_z b) = 0,$$

$$\partial_{tt}\eta - \mu\big(\lambda^2\partial_{xx} + \partial_{zz}\big)\eta = \tfrac{1}{4}\big(\lambda^2\partial_{xx} + \partial_{zz}\big)(b^2).$$

Recovers the KAW dispersion $\omega^2 = k_\parallel^2 v_A^2(1 + k_\perp^2\rho_s^2)$. (KAW equation: Hasegawa & Chen 1976; Shukla 1983. Forced acoustic response: Zakharov 1972; Karpman 1982.)

The $\frac{1}{4}(b^2)$ forcing is the **ponderomotive** drive (the wave's radiation pressure): plasma is expelled from regions of high intensity $|b|^2$.

Quasi-static (subsonic) closure: the strongly damped high-β slow mode is slaved to the wave intensity,

$$\eta = -\frac{1}{2(1+\beta)}\,|b|^2$$

(Mikhailovskii 1976; Stasiewicz 2000, Eq. 147)

3. Numerical method & validation

- 2-D Fourier **pseudospectral**, standard 2/3 dealiasing; **periodic** domain.
- **Exact** per-mode linear-oscillator propagator + Strang splitting of the nonlinear forcing; gentle spectral filter.
- Initial state: a **localized KAW packet** (amplitude A, perpendicular width $L_\perp$), then evolved freely.
- Fiducial: 128^2, box $100 \times 100\,\rho_s$, $\beta = 2$ ($\mu = 1$), $t = 0$–500 (≈ 80 ion-cyclotron periods); $\perp$ lengths in ρ_s, time in ω_{ci}^{-1}.
  Converged (checked at 256^2: slope identical, depth within $< 1\%$).

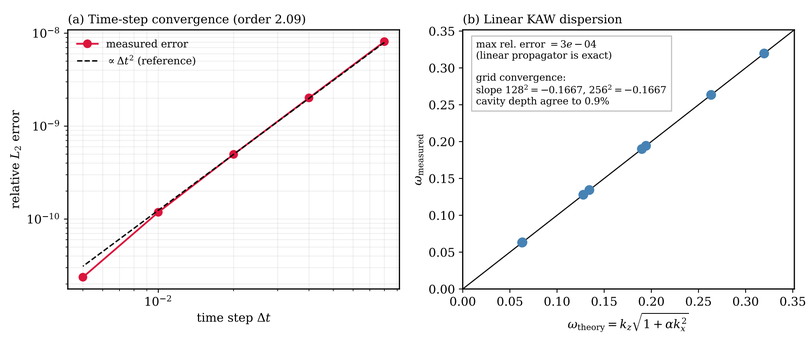

Figure 1: **Validation:** 2nd-order (Δt^2) time stepping (order 2.09); exact linear KAW dispersion (rel. error $\leq 3 \times 10^{-4}$); grid-converged.

4. MMS 2017-07-26 parameters

Measured plasma-sheet values $|B| \approx 17.4$ nT, $n_i \approx 0.16\,\mathrm{cm}^{-3}$, $\beta_i \approx 1.0$ ($\beta_{\mathrm{tot}} \approx 1.7$, **high-$\beta$**); hence $v_A \approx 2460$ km/s, $\rho_i \approx 420$ km, ion-cyclotron period $T_{ci} \approx 3.8$ s:

- Cavity size $\approx 20\,\rho_s \sim 8500$ km $\approx$ **1.3 Earth radii**.
- Lifetime $\geq 80\,T_{ci} \approx$ **5 minutes** (full run; nothing destroys it).
- Depth $\sim 10^{-3}$ at $|b| \leq 0.1$, extrapolating to $\sim 4\%$ at $|b| = 0.5$; deep holes lie beyond this linear response.

5. Cavity formation & mechanism

A localized KAW packet self-focuses into a **magnetic enhancement** with a co-located **density depletion**, a magnetic-hole-like cavity at ion scales ($\approx 20\,\rho_s$).

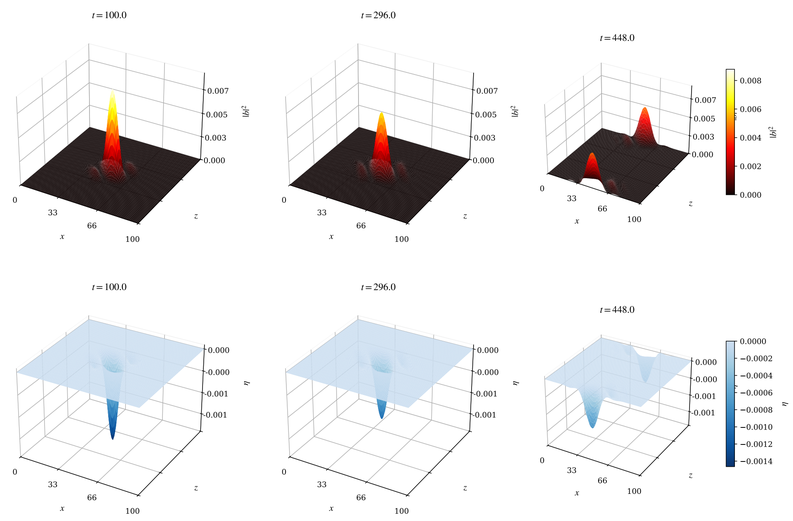

Figure 2: **3-D field evolution.**

The density falls on the ponderomotive line $\eta = -|b|^2/[2(1+\beta)]$: **expulsion from high-wave amplitude regions**.

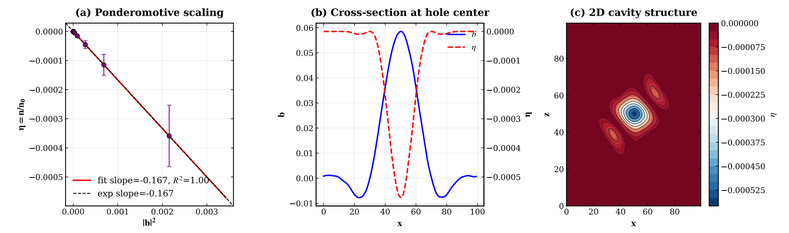

Figure 3: **Ponderomotive mechanism.**

6. Dynamic cavity, scaling & persistence

Fully dynamic two-field run (density evolved, *no* closure imposed): the same cavity forms and persists, the **independent** test of the mechanism.

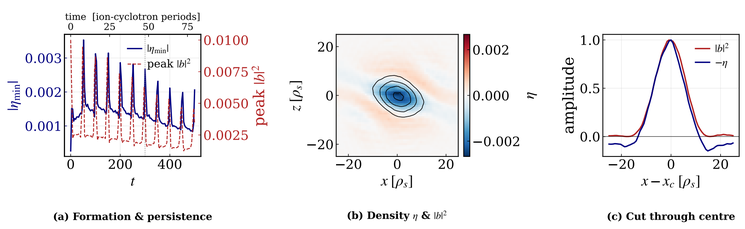

Figure 4: **Dynamic two-field cavity:** depth grows and persists; density minimum co-located with the $|b|^2$ maximum. In (c), $|b|^2$ and $-\eta$ are each normalized to unit peak.

The model also recovers the quasi-static high-β scaling $-1/(2\beta)$ **emergently** (ratio ≈ 1.1 for $\beta \geq 2$); at $\beta = 1$ the slaving breaks down, bracketing the regime of validity.

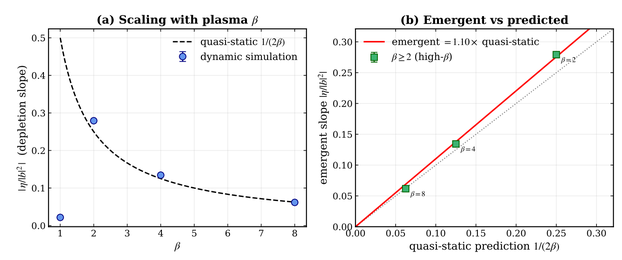

Figure 5: β**-scaling** (emergent, dynamic runs).

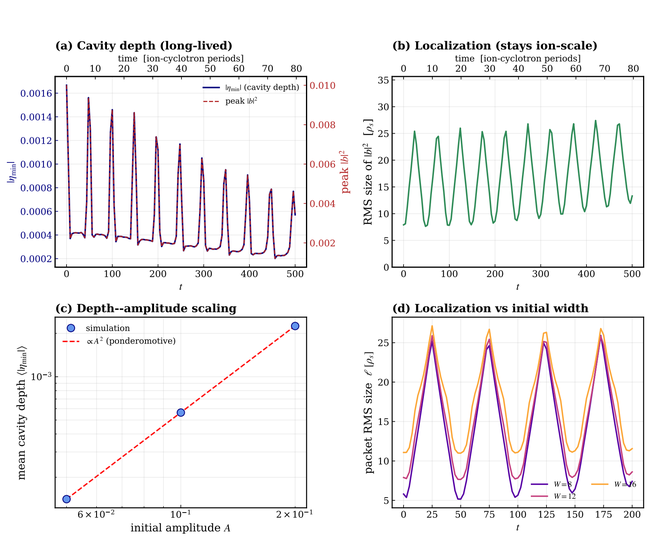

Figure 6: **Persistence & robustness:** cavity depth and size vs time; depth $\propto A^2$; localization across initial widths.

7. Observational comparison

- **Model ↔ data:** the model couples density to **KAW intensity** $|\delta B_\perp|^2$; in data this reads as density vs **total** $|B|$ via a compressive KAW ($|\delta B_\parallel|/|\delta B_\perp| \approx 0.45$) and pressure balance $\delta(B^2/2\mu_0) \approx -\delta p$: *low density where $|B|$ is high*. The linear slope is the pressure response, not the quadratic coefficient.
- **Mirror discriminator:** plasma-sheet holes are mirror-stable, 52/56 below $R_{\mathrm{m}} = (T_\perp/T_\parallel)/(1 + 1/\beta_\perp) = 1$, so the mirror mode cannot make most; our interval too ($R_{\mathrm{m}} \approx 0.35$).
- **MMS 2017-07-26** (independent crossing): $\beta_i \approx 1.0$ ($\beta_{\mathrm{tot}} \approx 1.7$), anti-correlation $r = -0.18$ ($N = 3460$), and $\delta E_\perp/(\delta B_\perp v_A) \approx 1.8$, kinetic Alfvén waves at $\rho_i \approx 420$ km.

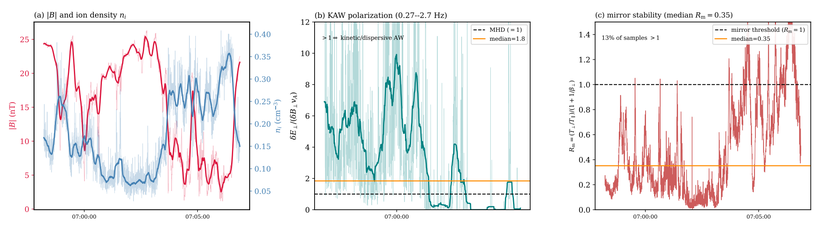

Figure 7: **MMS plasma sheet** (2017-07-26): $|B|$–n_i anti-correlation, kinetic-Alfvén polarization, and mirror stability.

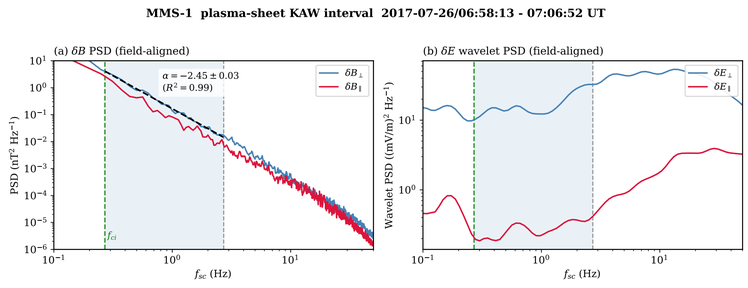

Figure 8: **Spectra** (field-aligned): $\delta B_\perp$ dominates with kinetic-range slope -2.45, and $\delta E_\perp \gg \delta E_\parallel$ across the KAW band: broadband kinetic Alfvénic turbulence rather than a single coherent wave.

Not just one window: the same pipeline across the available magnetotail KAW intervals (windows set by burst-segment boundaries, not tuned); the 2017-05-31 set is a separate, previously reported PSBL crossing (Zhang+ 2022):

interval	β_i	$\delta E_\perp/(\delta B_\perp v_A)$	$r(\delta n, \delta B)$
2017-07-26 (independent)	1.01	1.8	-0.18
2017-05-31 PSBL (central)	0.54	5.1	-0.25
2017-05-31 approach (lobe-like)	0.16	8.7	-0.04
2017-05-31 PSBL (following)	0.43	4.8	-0.10

The observed density–magnetic anti-correlation is consistent with the ponderomotive mechanism, but is not by itself a unique proof of it.

8. Conclusions

- KAW–slow-mode **ponderomotive coupling** generates **long-lived, ion-scale density cavities** with the observed density–magnetic anti-correlation.
- In the **fully dynamic two-field system** (no closure imposed) the cavity forms, stays co-located, and **persists**, and the depletion scaling emerges unimposed, the independent test of the mechanism.
- Depth follows the quasi-static law $\eta = -|b|^2/[2(1+\beta)]$; weakens with β, explaining weak high-β holes.
- Consistent with plasma-sheet magnetic holes (Sun 2012) and Alfvénic density cavities (Stasiewicz 2000): a **viable mechanism** for hole-like cavities in high-β magnetotail environments.

Selected references

1. Zakharov (1972) *Sov. Phys. JETP* **35**, 908.
2. Mikhailovskii, Petviashvili & Fridman (1976) *JETP Lett.* **24**, 43.
3. Hasegawa & Chen (1976) *Phys. Fluids* **19**, 1924.
4. Karpman (1982) *J. Plasma Phys.* **27**, 215.
5. Shukla (1983) *Phys. Rev. A* **27**, 1702.
6. Stasiewicz et al. (2000) *Space Sci. Rev.* **92**, 423.
7. Wygant et al. (2002) *J. Geophys. Res.* **107**, 1201.
8. Sun et al. (2012) *Ann. Geophys.* **30**, 583.
9. Zhang et al. (2022) *Earth Planet. Phys.* **6**, 465.
10. Chettri et al. (2024) *Res. Astron. Astrophys.* **24**, 105009.

Data

MMS (FGM/FPI/EDP) via the MMS Science Data Center and CDAWeb, analyzed with PySPEDAS. Contact: MK Chettri, Sikkim University (mkchettri8@gmail.com).